

# Large-Scale Ocean Heat and Freshwater Transports during the World Ocean Circulation Experiment

ALEXANDRE GANACHAUD

*Laboratoire d'Etudes Géophysiques et d'Océanographie Spatiale  
Institut de Recherche pour le Développement, Nouméa, New Caledonia*

CARL WUNSCH

*Department of Earth, Atmospheric, and Planetary Sciences, Massachusetts Institute of Technology, Cambridge, Massachusetts*

(Manuscript received 9 November 2001, in final form 18 June 2002)

## ABSTRACT

Hydrographic sections obtained during the World Ocean Circulation Experiment are combined using a geostrophic inverse model to estimate the global-scale horizontal transports and transport divergences of heat and freshwater with self-consistent error bars. The overall results are compared to bulk formula-derived climatologies and estimates derived from atmospheric reanalyses. At 7.5°N in the Atlantic, a previous estimate of the heat transport is modified. A recent atmospheric residual estimate from NCEP and the Earth Radiation Budget Experiment (ERBE) products is consistent with the present results for the heat budget, except at high northern latitudes where it falls outside error estimates. The freshwater transport divergence from hydrography is statistically significant only when integrated over very large areas and difficult to test—as extant climatological estimates differ substantially from each other. Hydrographic estimates can be improved through repeated observations to reduce the temporal aliasing, and by combining more detailed regional estimates using more data types. To permit a formal comparison and assimilation in ocean general circulation models, atmospheric estimates urgently require convincing error estimates for both heat and freshwater transports.

## 1. Introduction

Four main methods have been used to estimate heat exchanges between the ocean and atmosphere. 1) Calculation of the lateral transport within the ocean from determination of the general circulation. Any transport divergence of either sign is absorbed or provided by the atmosphere. This method will be called the “hydrographic” one. 2) Calculation of the transports within the atmosphere from determination of its general circulation by models constrained with the extensive atmospheric observation networks. Ocean–atmosphere heat fluxes are determined at the lower boundary, during model integration, and based on parameterizations of the model variables. These values are generated along with operational products, and will be referred to as lower boundary conditions (LBC). 3) Any energy transport divergence from atmospheric reanalyses is either radiated to space or absorbed/provided by the ocean. The radiation to space is accurately determined by satellite measurements [the Earth Radiation Budget Ex-

periment (ERBE)] and the residual corresponds to heat exchanges with the oceans (e.g., Trenberth and Caron 2001, hereafter TC). We will refer to such estimates as those from “atmospheric residuals.” The residual method differs from method 2 because of the constraint to compatibility with measured radiation to space. In both methods 2 and 3, the atmospheric circulation is determined using all the atmospheric observations with physical constraints from an assimilating model. 4) Air–sea transfers calculated from bulk formulas using local observations as done in method 2 with the fields from the reanalyses. Interpreted as a transport divergence of the ocean, they can be integrated to produce an oceanic lateral flux. These will be called the “bulk formula” estimates. These different methods are complementary and serve different purposes in the context of climate modeling and observation. We summarize here their strengths and weaknesses before comparing the derived transoceanic heat transports from methods 2–4 with those from method 1.

The bulk formula calculation uses data from voluntary observing ships and buoys (e.g., Josey et al. 1999); the comparatively large existing database permits production of monthly climatologies. Nevertheless, these products suffer from poor data distribution in both time

---

*Corresponding author address:* Dr. Alexandre Ganachaud, Institut de Recherche Pour le Développement, Nouméa, B. P. A5, 98848 Nouméa Cedex, New Caledonia.  
E-mail: Alexandre.Ganachaud@noumea.ird.nc

and space, with most of the data lying along the main shipping routes. In addition, the bulk formulas are of questionable accuracy, for example, at high wind speeds. Large-scale integration of small systematic errors results in biases that can reach 10 PW (1 PW =  $10^{15}$  W; e.g., Josey et al. 1999; Taylor 2000) over the global ocean.

LBC and “residual” products depend on the accuracy of horizontal heat transport divergences provided by data-assimilating atmospheric models in reanalyses. Despite their constraints by atmospheric data, these estimates exhibit problems such as strong imbalances over land and/or finite net global heat flux to the ocean (Keith 1995; Garnier et al. 2000; TC). Thus, ad hoc adjustments, intended to render the results physically sensible, are made to the apparent over-ocean fluxes. Because of their high resolution, these products are attractive to modelers, but their accuracy—which compounds the complex uncertainties of the data and the model integration with that of the adjustments—is impossible to calculate directly. For example, TC estimate uncertainties empirically, based on a comparison (Trenberth et al. 2001) of the European Centre for Medium-Range Weather Forecasts (ECMWF) and the National Centers for Environmental Prediction–National Center for Atmospheric Research (NCEP–NCAR) reanalyses with each other and with bulk formula products, that suggested uncorrelated constant-with-latitude random errors. Such estimates may well grossly underestimate the true uncertainties as ECMWF and NCEP reanalyses are based upon similar observation networks and parameterizations. (A referee argues that the uncertainties are “known perfectly over land and pretty well over the ocean.” The reader must judge.) The resulting TC estimates of meridional oceanic heat transports deviate much more from each other than is consistent with the inferred error bars in the Southern Ocean—a contradiction suggesting an underestimate of the true errors. In their evaluation, TC suggested that the NCEP-derived estimate was globally more reliable than the ECMWF one (see their discussion p. 3435).

Air–sea exchanges of freshwater, that is, evaporation and precipitation, are a second extremely important class of climate variable. Despite their key role in climate regulation, freshwater transport estimates are highly uncertain. Wijffels (2001) compared 13 different freshwater products and found 100% differences between many of them. Evaporation is estimated from empirical formulas, based on either in situ observations or satellite radiometers. Precipitation is more difficult to estimate because the data distribution over the ocean is sparse, and temporally sporadic. Satellite microwave and outgoing longwave radiation sensors provide estimates for integral properties of water drops and ice particles that can be related to precipitation. The relations used, however, are affected by many factors and, lacking appropriate calibration data, result in highly uncertain estimates. Adler et al. (2001) found that “quasi-standard”

zonally integrated precipitation estimates deviated from each other by a factor of 2.

Freshwater estimates from atmospheric reanalyses are dynamically more consistent, although they too suffer from the lack of oceanic data and from the difficult parameterization of cloud physics. Trenberth and Guillemot (1998) use a residual method similar to the one for heat and, based on the NCEP reanalysis, to estimate the net freshwater exchanges with the ocean from the divergence of horizontal moisture transports. They found strong systematic differences with other freshwater products, including the NCEP LBC evaporation and precipitation. Discrepancies were particularly important in the Tropics where wind divergence (from NCEP in that case) is thought to be particularly uncertain. Local air–sea freshwater exchanges can also be obtained from bulk formulas, involving again a complex error estimation problem (Taylor 2000). As with heat, bulk formula estimation of the freshwater budget suffers from the accumulation of errors on large scales.

The focus here is upon the time-mean transoceanic heat and freshwater transport estimates as obtained from the World Ocean Circulation Experiment (WOCE) observations. A major goal of WOCE was the production of the best possible estimates of oceanic transports of climatologically important variables. A preliminary version of the global heat transport results was presented by Ganachaud and Wunsch (2000). Here we discuss regional variations and mechanisms of transport, modify the previously estimated North Atlantic heat transport value at  $7.5^{\circ}\text{N}$ , and provide estimates with uncertainties of the air–sea freshwater exchanges. [The transports and divergences of other climatologically important variables—specifically oxygen and nutrients—are discussed by Ganachaud and Wunsch (2002).]

## 2. Data and model

Our hydrographic estimates are based on the selected hydrographic WOCE and associated program sections of Fig. 1. The method is that of inverse box models (Wunsch 1996): across each hydrographic section, a high-resolution geostrophic velocity field is determined so that the circulation satisfies near-conservation of several properties including mass, salt, and heat. Near-conservation is required where appropriate, between the sections, and within oceanic layers (Fig. 2) bounded by isopycnal, or “neutral” surfaces (Jackett and McDougall 1997). Vertical advective and diffusive property transports are calculated between the layers. Heat conservation is required only within layers that are not in contact with the surface. The circulation includes the directly wind-driven (Ekman) transports near the surface, with an initial value based on the NCEP reanalysis (Kalnay et al. 1996). The solution for the global, time-mean circulation consists of horizontal velocities across the sections; vertical advection and diffusion between layers; an adjustment to the initial Ekman transport and

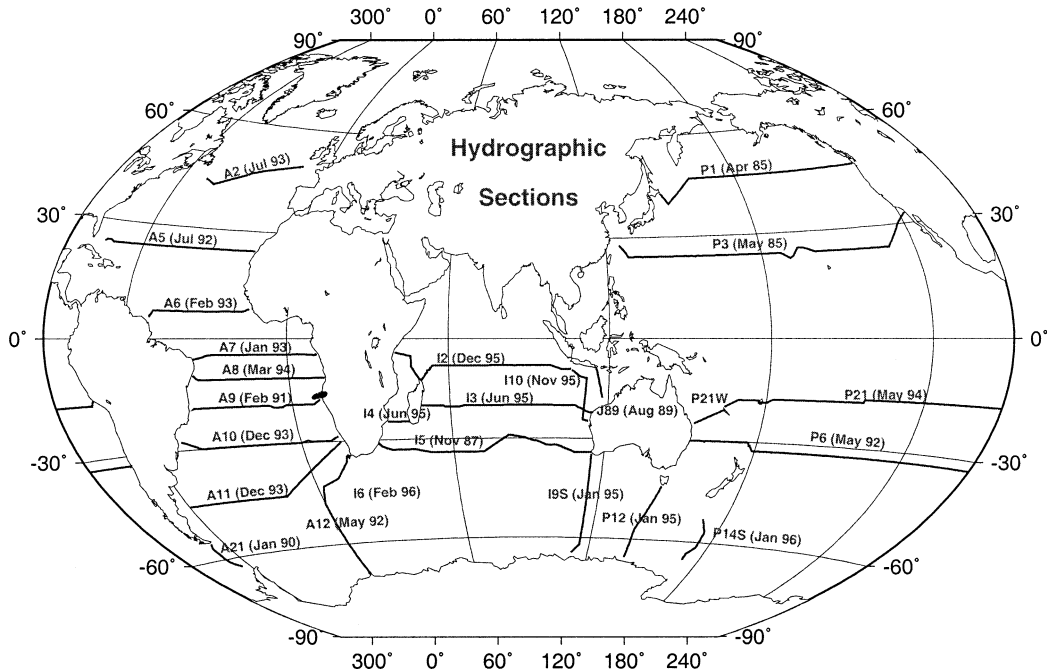


FIG. 1. Hydrographic sections used in the box inverse method. Transoceanic sections were selected from the WOCE and JADE experiments to ensure a reasonable temporal consistency [1990–96, except in the North Pacific (1985) and south Indian (1987) Oceans]. Each section is a collection of high-density temperature, salinity, oxygen, and nutrients measurements. Only zonal (meridional in the Southern Ocean) sections are used to avoid the large potential noise sources that arise when sections cross each other at different times.

the net freshwater transports—including evaporation, precipitation, and river runoff in each oceanic box between sections. A full error covariance of the solution is available, permitting a thorough uncertainty calculation for the derived quantities such as heat (energy) transports and divergences. More details of the data and model can be found in Ganachaud and Wunsch (2000), Ganachaud et al. (2000), and Ganachaud (2002, manuscript submitted to *J. Atmos. Oceanic Technol.*, hereafter GAN).

The uncertainties that we report include those for Ekman transport, which were set to 50% of the initial value—a conservative estimate—and the model error, which is dominated by the aliasing of oceanic variability

in the synoptic sections that are sampled in different years and seasons. The effect of oceanic variability was estimated, along with other errors, by GAN from a high-resolution numerical ocean model. Because, away from the equator, the major oceanic variability reflects a balance between surface Ekman transport and a depth-independent return flow, the impact on hydrographic measurements is reduced and the time-mean transports are estimated with relative accuracy as long as one uses the time-mean Ekman transport at the surface. Correlated temporal variations in the temperature field (rectification) are not directly taken into account, and numerical simulations suggest this effect is small (Jayne and Marotzke 2001).

One consequence of those error sources is that no conservation equation, including mass, should be satisfied exactly, and residual imbalances are always present. Mass imbalances are confirmed to be indistinguishable from zero within error bars. However, to decrease the effects of the small remaining residuals on air–sea heat and freshwater divergences, the latter are calculated in an anomaly form (McDougall 1991). The resulting property *divergences* are exactly mass and salt conserving, in contrast to the horizontal transports, which are uncorrectable this way. (At 7.5°N, the extremely high noise in the net transport led us to adjust the heat transport value using the mass-conserving divergence between 24° and 7.5°N, as described below.)

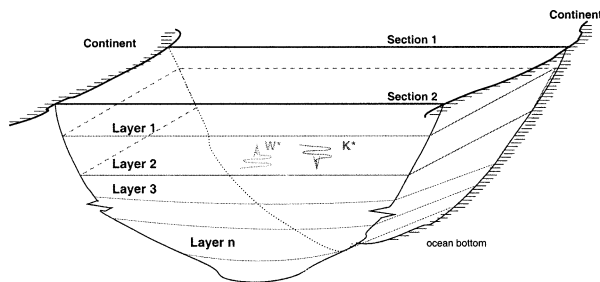


FIG. 2. Inverse model structure. The velocity field across hydrographic sections is estimated so that conservation requirements are met within isopycnal layers, bounded by neutral surfaces. Advective and diffusive exchanges are allowed between layers.

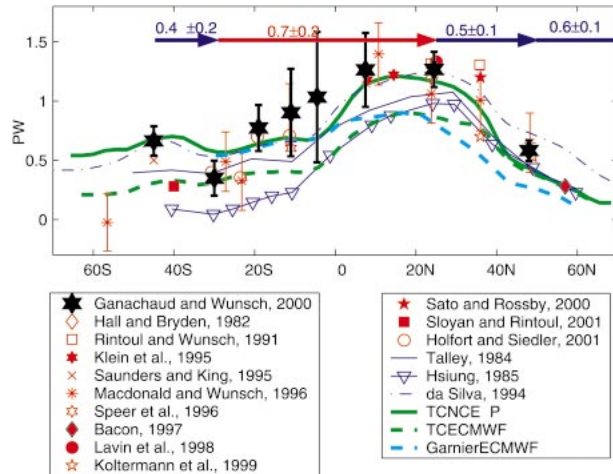


FIG. 3. Atlantic Ocean heat transports. Black stars with thick error bars indicate advective horizontal heat transports across hydrographic sections—except at  $7.5^{\circ}\text{N}$ , see text—numbers above the arrows indicate the divergences, or air–sea fluxes, positive/red for ocean heat gain, negative/blue for ocean heat loss. Heat, or energy transports are referred to  $0^{\circ}\text{C}$ . Error bars on other hydrographic estimates (red symbols) are, respectively,  $\pm 0.3$  PW (Hall and Bryden 1982);  $\pm 0.2$  PW (Rintoul and Wunsch 1991);  $\pm 0.1$  PW (Saunders and King 1995);  $\pm 0.17$  PW (Speer et al. 1996);  $\pm 0.06$  (Bacon 1997);  $\pm 0.26$  (Lavin et al. 1998);  $\pm 0.15$  PW (Koltermann et al. 1999);  $\pm 0.3$  PW (Sato and Rossby 2000);  $\pm 0.04$  PW (Sloyan and Rintoul 2001); and  $\pm 0.3$  PW (Holfort and Siedler 2001) all taken at face value. Also shown are heat transport estimates grouped by method: bulk estimates (blue), atmospheric residuals (green), and LBC of atmospheric reanalyses (dashed cyan). Northward heat transport is positive. In general, if one confines attention only to estimates accompanied by error bars, they are now consistent within one standard error.

The circulation, property transports, and uncertainties may therefore be regarded as time averages over the period spanned by the dataset, that is, approximately 1985–96, with the 1985 sections being confined to the North Pacific.

### 3. Heat transports

We use “heat transport” as a shorthand for what is really an energy transport (see Warren 1999). Figure 3 shows our estimate of horizontal oceanic heat transports and their (mass conserving) divergences, along with estimates from previously published work using hydrography and climatologies in the Atlantic. Numerical values for the present study are listed in Table 1. There is a surface warming of  $0.7 \pm 0.2$  PW ( $18 \pm 5 \text{ W m}^{-2}$ ) in the Tropics, a cooling of  $-1.1 \pm 0.14$  PW in the north, and  $-0.4 \pm 0.2$  PW in the south between  $30^{\circ}\text{S}$  and WOCE section A11, at approximately  $45^{\circ}\text{S}$ . [the convention here is that a positive divergence is oceanic heat gain, and a negative divergence (i.e., convergence) is a heat loss.]

Uncertainties vary with latitude, with an increase toward the equator, but the heat transport values are significantly different from zero everywhere. The net transport at  $7.5^{\circ}\text{N}$  was originally estimated as  $1 \pm 0.55$  PW

TABLE 1. Meridional oceanic heat transport, positive northward.

Region	Latitude*	Heat transport**
Atlantic	$47^{\circ}\text{N}$	$0.6 \pm 0.09$
	$24^{\circ}\text{N}$	$1.27 \pm 0.15$
	$7.5^{\circ}\text{N}$	$1.26 \pm 0.31$
	$4.5^{\circ}\text{S}$	$1 \pm 0.55$
	$11^{\circ}\text{S}$	$0.9 \pm 0.4$
	$19^{\circ}\text{S}$	$0.77 \pm 0.2$
	$30^{\circ}\text{S}$	$0.35 \pm 0.15$
Indo-Pacific	$45^{\circ}\text{S}$	$0.66 \pm 0.12$
	$47^{\circ}\text{N}$	$0 \pm 0.05$
	$24^{\circ}\text{N}$	$0.52 \pm 0.2$
	$18^{\circ}\text{S}$	$-1.6 \pm 0.6$
	$30^{\circ}\text{S}$	$-0.9 \pm 0.3$
Global	$47^{\circ}\text{N}$	$0.6 \pm 0.1$
	$24^{\circ}\text{N}$	$1.8 \pm 0.3$
	$19^{\circ}\text{S}$	$-0.8 \pm 0.6$
	$30^{\circ}\text{S}$	$-0.6 \pm 0.3$

\* Latitudes are nominal; see Fig. 1 for exact location.

\*\* Units are  $\text{PW} = 10^{15} \text{ W}$ .

(Ganachaud and Wunsch 2000). Because that section crosses the region of high variability of the North Brazil Current at low latitudes ( $6^{\circ}\text{N}$  on the western end), it is subject to high measurement noise and strong aliasing of oceanic variability, thus, mass was not conserved in the solution in this region. In addition, the section does not sample the part of the current on the continental shelf, a part that was estimated as having a mass transport of about  $5 \text{ Sv}$  ( $1 \text{ Sv} \equiv 10^6 \text{ m}^3 \text{ s}^{-1}$ ) at  $26^{\circ}\text{C}$  (Lux and Mercier 2001) and added here. Because the heat transport is more accurately determined at  $24^{\circ}\text{N}$ , where the data are less subject to aliasing and other errors, we have modified the original transport estimate at  $7.5^{\circ}\text{N}$ . In its place the estimated heat divergence between  $24^{\circ}$  and  $7.5^{\circ}\text{N}$  is subtracted from the  $24^{\circ}\text{N}$  transport to provide a new estimate at  $7.5^{\circ}\text{N}$ . Because as computed, the heat divergences are mass conserving, this corrected value is believed to be more accurate. Only the  $7.5^{\circ}\text{N}$  value was modified this way because mass residuals in the upper-ocean layers implied a large difference between the  $7.5^{\circ}$  and  $24^{\circ}\text{N}$  horizontal transports and the anomaly divergence.

The previous global inverse model estimates of Macdonald and Wunsch (1996, hereafter MW96), based on older hydrographic data spanning 30 yr before WOCE, fall within 1–1.3 standard deviations of our estimates. Early regional hydrographic estimates of Hall and Bryden (1982) and Rintoul and Wunsch (1991), based on a single and two pre-WOCE sections in the North Atlantic, respectively, are also in agreement, so that no changes in time of the heat transports can be detected at the present level of uncertainty. The Klein et al. (1995) estimate in the Tropics agrees closely with ours. Lavin et al. (1998) reached a similar conclusion—of no distinguishable temporal change—after comparing three repeated sections at  $24^{\circ}\text{N}$ . Regional estimates obtained during the WOCE period are consistent with ours, too

(Sloyan and Rintoul 2001; Saunders and King 1995; Holfort and Siedler 2001; Speer et al. 1996; Lavin et al. 1998; Koltermann et al. 1999). These are all at least partially based on the same data and used similar constraints; but because they are regional, there is no guarantee that the estimates are mutually consistent.

Heat transports from the bulk formula climatologies of Talley (1984) and Hsiung (1985) also indicated in Fig. 3, are generally lower than the hydrographic ones by 0.2–0.5 PW, suggesting that they may underestimate the ocean heat loss in the North Atlantic. In contrast, the da Silva et al. (1996) climatology, also from bulk formulas, produces a heat loss that is larger than ours north of 47°N, and smaller between 24° and 47°N. The bulk formula estimates are thus themselves not consistent. To the south, Hsiung's climatology overestimates ocean warming in the Tropics and underestimates cooling in the northern subtropics.

In Fig. 3 the heat transports of TC are also reported from the atmospheric residual method based on the NCEP and ECMWF horizontal atmospheric heat transports. The NCEP-derived estimate (hereafter, the two estimates will be called TC-NCEP and TC-ECMWF) is lower than ours by 0.15 PW at 47°N—exceeding our 0.1 PW error bar. This difference contributes to a lower heat transport over the whole Atlantic basin while ocean–atmosphere heat exchanges (divergences) are consistent with the hydrography between 47°N and 19°S. [The need for a finite high-latitude North Atlantic northward export of heat is made visually apparent in plates 44 and 48 in Worthington and Wright (1970), displaying the striking midwinter poleward flux of warm water at 53° and 60°N and the intense, very cold return flow there.]

The TC-NCEP estimate also shows the cooling that we find between 45° and 30°S although there the comparison is limited by the different areas of integration because the WOCE section at 45°S is not zonal. The TC-ECMWF residuals produce weak cooling in the North Atlantic. If one attributes an uncertainty to the TC-ECMWF, heat transports which is no smaller than the difference between TC-NCEP and TC-ECMWF, there is no formal contradiction between TC-ECMWF results and our results.

Also plotted in Fig. 3 is the Garnier et al. (2000) estimate from the LBC of ECMWF Re-Analysis, globally adjusted to have no net ocean heat gain. Although these northern values are close to those of TC-ECMWF, they diverge substantially in the Tropics (0.25 PW)—an alarming deviation—as both products are derived from the same reanalysis, and are used to force ocean general circulation models. Hydrographic estimates at 14.5°, 36°, and 55°N are higher than other products as well. [The Bacon (1997) estimate is for net transport between Greenland and England, and is nonzonal from 55° to 60°N.]

In the Pacific and Indian Oceans, the database is much sparser, and additional uncertainties arise because of the

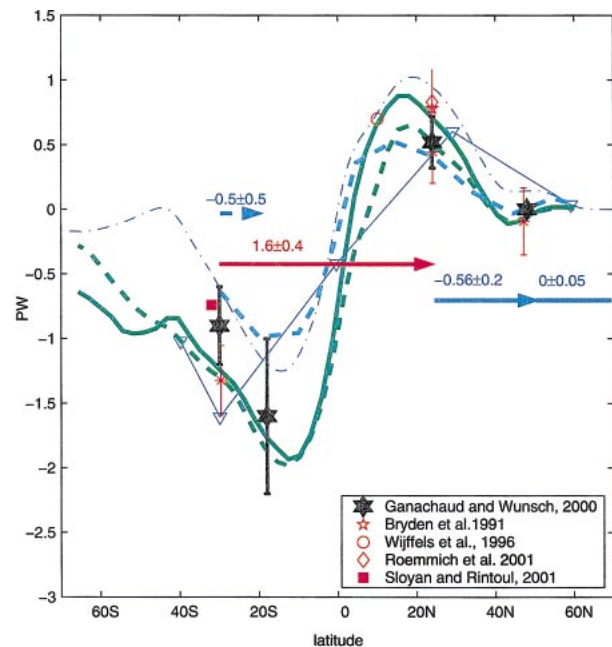


FIG. 4. Same as Fig. 3, but for the summed Indian and Pacific Oceans heat transports.

poorly determined energy transport through the Indonesian archipelago. In the present model, the Indonesian Throughflow transport (ITF) estimate is heavily dependent on the single 1989 hydrographic Java–Australia Dynamic Experiment (JADE) section that was used, and is therefore subject to seasonal bias in a region of high variability. (A 1992 occupation did not contain the nutrient data necessary to adequately constrain the model.) To circumvent the uncertainty introduced by the ITF, we summed the heat transport of the Pacific and Indian Oceans (Fig. 4). Because other regional estimates produced different values of ITF, only the Sloyan and Rintoul (2000) and MW96 estimates could be summed consistently in the Southern Hemisphere. Surprisingly, the Sloyan and Rintoul (2000) estimate agrees with ours, although their inverse model produces a much larger influx of deep water out of the Southern Ocean. The MW96 estimates are a bit lower, although not statistically distinguishable. Among the many differences between the MW96 model and ours is their use of the early Scorpio data (1968, Stommel et al. 1973) versus our WOCE section of 1992. In the subtropical North Pacific, both Bryden et al. (1991, single occupation) and Roemmich et al. (2001, repeated upper-ocean data) yield a higher heat transport than either ours or that of MW96. The Roemmich et al. (2001) estimate takes full advantage of the large number of measurements; but there is no guarantee that the resulting circulation is compatible with other regions; in contrast, we use a single synoptic section in a globally compatible circulation. At this point we cannot discriminate between the two values,

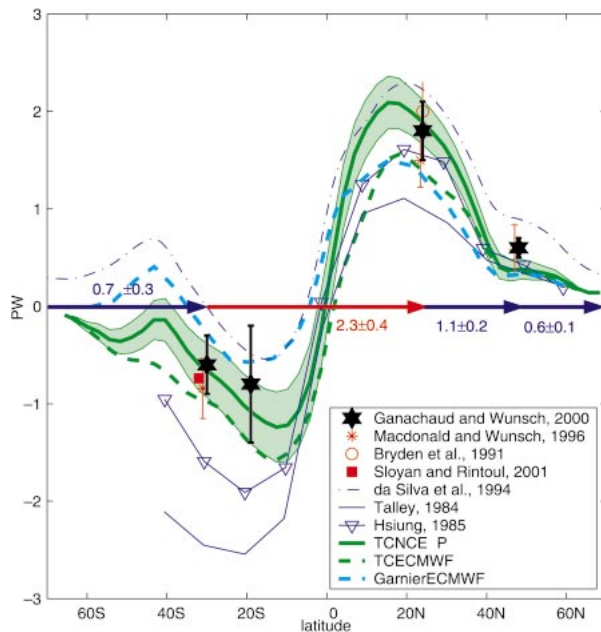


FIG. 5. Same as Fig. 3, but for the global ocean. The green band indicates the uncertainty estimated heuristically by TC.

whose error bars do overlap for a nominal solution range of 0.55–0.70 PW.

In the Indo-Pacific region, climatologies give very divergent results, with an extreme difference of 0.75 PW between da Silva and TC-NCEP at 40°S. The discrepancies are related to the lack of in situ observations in the south Indian and Pacific Oceans. As in the Atlantic, both TC estimates are in close agreement with ours. TC-NCEP, TC-ECMWF, and MW96 exhibit a net heating that is higher than ours between 24°N and 30°S. Also note the large deviation there between the TC-ECMWF and the LBC-ECMWF of Garnier et al. (2000)—a 0.9-PW difference.

Globally (Fig. 5), one sees a considerable asymmetry across the equator. The small poleward transport in the Southern Hemisphere is the result of near-cancellation of the vigorous northward transport in the South Atlantic, with the net southward transport in the combined Indo-Pacific Oceans. Estimated ocean heating is  $2.3 \pm 0.4$  PW in the tropical band; 70% of the corresponding cooling takes place north of 24°N ( $-1.7 \pm 0.25$  PW) and 30% in the Southern Ocean ( $-0.7 \pm 0.3$  PW). Those air–sea fluxes are consistent with previous hydrographic estimates. The TC-NCEP estimates are similar to that of hydrography except at 47°N, where hydrographic estimates suggest that the TC estimate is too low by 0.2 PW.

Both ECMWF oceanic heat transport values from TC and Garnier are lower than the TC-NCEP ones in the northern Tropics, as noted by TC. In the Southern Hemisphere, both residual analyses by TC from NCEP and ECMWF are consistent with observation, while the ECMWF values from Garnier et al. (2000) produce

much lower air–sea exchanges. On the whole, however, the NCEP residual analysis is closest to the hydrographic inversion estimate.

#### 4. Freshwater

We now examine the inverse model-estimated freshwater divergences. Net ocean–atmosphere freshwater exchanges over large oceanic areas can be derived from the mass and salt budgets between hydrographic sections. Because freshwater exchanges are small fractions of large horizontal mass transports, the noise in the mass budget is much larger than the freshwater divergences. To obtain meaningful freshwater divergences, one has to make use of the assumed strong correlation between mass and salt transport. The corresponding conservation equations are

$$\nabla \cdot \rho \mathbf{v} + n_M + F = 0, \quad (\text{mass})$$

$$\nabla \cdot (\rho \mathbf{v} S) + n_S = 0, \quad (\text{salt})$$

$$\nabla \cdot \left[ \rho \mathbf{v} \left( 1 - \frac{S}{\bar{S}} \right) \right] + n' + F = 0, \quad (\text{salt anomaly}),$$

where the third equation follows from subtracting  $1/\bar{S}$  times the second equation from the first. Here  $\mathbf{v}$  is velocity,  $S$  is salinity,  $\bar{S}$  is an average salinity, and  $n_M$  is the noise in the mass conservation equation and  $n_S$  is the noise in the salt. The first term of the last equation is the divergence of the transport of salt anomaly and  $F$  is the net freshwater input to the area. Here  $n' = n_M - n_S/\bar{S}$  is thought to have a magnitude about one order of magnitude smaller than  $n_M$  (Wunsch 1996; Wijffels 2001). The  $F$  is estimated as part of the inverse solution.

Figure 6 shows the net freshwater air–sea flux diagnosed from the global hydrographic model compared with several types of climatologies from the Wijffels (2001) compilation (values are listed in Table 2). By net freshwater flux is meant  $P + R - E$ , with  $E$ ,  $P$ , and  $R$  being evaporation, precipitation, and runoff, respectively. Wijffels (2001) used the Baumgartner and Reichel (1975) estimate for runoff, as it appeared to be closest to the net  $P - E$  balance over land, but as she pointed out, runoff errors are a large additional source of uncertainty in the oceanic freshwater budget. After inversion, the uncertainty is still close to 100% of the freshwater transports, and values are meaningful only when integrated over large areas, accounting for the correlated errors. For instance, in the whole Atlantic Ocean between 30°S and 47°N, the integral amounts to  $0.5 \pm 0.3$  Sv (net evaporation). All estimates suggest that the tropical oceans are evaporative, except the tropical Pacific where freshwater is indistinguishable from balance ( $P + R - E \approx 0$ ). In the North Atlantic, the inverse model suggests a similar near-balance, with large uncertainties, whereas climatologies all indicate evaporation of about 0.2 Sv. Freshwater is close to balance in the North Pacific as well. In the southern subtropical

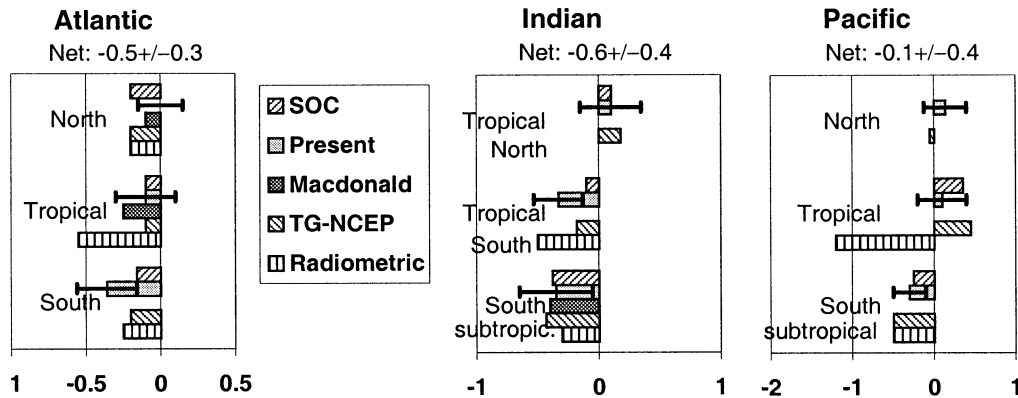


FIG. 6. Freshwater divergences ( $30^{\circ}\text{S}$ – $47^{\circ}\text{N}$ ) from the hydrographic inverse model (“present”) in units of  $10^9 \text{ kg s}^{-1}$  ( $\approx \text{Sv}$ ). Overlain are, based on the review by Wijffels (2001), the bulk formula climatology of Josey et al. [1999; Southampton Oceanography Centre (SOC)], the previous inverse model of Macdonald (1998); the residuals derived from NCEP reanalysis of Trenberth and Guillemot (1998) and radiometric data (Jourdan et al. 1997). The river runoff estimates of Baumgartner and Reichel (1975) are added to the last two estimates. Negative numbers indicate net evaporation; positive numbers indicate net precipitation/river runoff. In the Atlantic and Pacific Oceans, latitude ranges are roughly  $30^{\circ}$ – $18^{\circ}\text{S}$  (south),  $18^{\circ}\text{S}$ – $24^{\circ}\text{N}$  (tropical), and  $24^{\circ}$ – $47^{\circ}\text{N}$  (north); while in the Indian Ocean, the ranges are  $32^{\circ}$ – $18^{\circ}\text{S}$  (south subtropics),  $18^{\circ}$ – $8^{\circ}\text{S}$  (south tropical), north of  $8^{\circ}\text{N}$  (north tropical). Numbers above the graphs give the net sum between  $30^{\circ}\text{S}$  and  $47^{\circ}\text{N}$  for each ocean.

regions of all three oceans, all climatologies indicate evaporation with similar magnitudes, in agreement with the inverse model results. Generally, climatologies give freshwater fluxes of the same magnitudes, but the estimates derived by Jourdan et al. (1997) from satellite radiometric data show much larger tropical evaporation estimates, beyond our error bars, suggesting a systematic error somewhere. In all other regions, there is consistency between our results and climatologies (error bars are only one standard deviation). The global ocean over  $30^{\circ}\text{S}$ – $47^{\circ}\text{N}$  is evaporative, with a loss of  $1.2 \pm 0.5 \text{ Sv}$ . In the Southern Ocean, we estimate an uncertain net precipitation/runoff of  $0.8 \pm 0.9 \text{ Sv}$ . Closure of the world freshwater budget would therefore imply an additional  $0.4\text{-Sv}$  precipitation north of  $47^{\circ}\text{N}$ , in agreement with most climatologies.

## 5. Transport processes

Understanding the process by which the ocean transports heat and freshwater is an important issue in climate

TABLE 2. Ocean–atmosphere freshwater exchanges. Positive is precipitation/river runoff.

Region	Latitude range*	Freshwater flux**
Atlantic	$47^{\circ}$ – $24^{\circ}\text{N}$	$0 \pm 0.15$
	$24^{\circ}\text{N}$ – $19^{\circ}\text{S}$	$-0.1 \pm 0.2$
	$19^{\circ}$ – $30^{\circ}\text{S}$	$-0.36 \pm 0.2$
Indian	North– $8^{\circ}\text{S}$	$0.1 \pm 0.25$
	$8^{\circ}$ – $20^{\circ}\text{S}$	$-0.33 \pm 0.2$
	$20^{\circ}$ – $32^{\circ}\text{S}$	$-0.35 \pm 0.3$
Pacific	$47^{\circ}$ – $24^{\circ}\text{N}$	$0.14 \pm 0.26$
	$24^{\circ}\text{N}$ – $17^{\circ}\text{S}$	$0.1 \pm 0.3$
	$17^{\circ}$ – $30^{\circ}\text{S}$	$-0.3 \pm 0.2$

\* Latitudes are nominal; see Fig. 1 for exact location.

\*\* Units are  $10^9 \text{ kg s}^{-1}$ .

modeling, as an incorrect partitioning would lead to incorrect sensitivities. Several authors, for example, Bryden and Imawaki (2001), suggest a decomposition of the heat transport into three parts from the net mass transport, the meridional overturning, and the integrated effects of horizontal circulations, so that the heat budget is

$$\begin{aligned}
 H &\doteq \iint dx dz \rho c_p \theta v \\
 &= \langle \bar{v} \rangle^x \langle \overline{\rho c_p \theta} \rangle^x \int dz L(z) + \int dz L(z) \langle v \rangle^x \langle \rho c_p \theta \rangle^x \\
 &\quad + \iint dx dz (\rho c_p \theta)' v', \quad (1)
 \end{aligned}$$

where  $c_p$  is the heat capacity,  $x$  is the horizontal coordinate along the section,  $z$  is the vertical coordinate,  $L(z)$  is the length of a zonal section at each level,  $\langle \cdot \rangle^x$  is the zonal average, and  $\langle \bar{\cdot} \rangle^x$  is the zonal and depth average and the prime indicates the remaining deviations with

$$v(x, z) = \langle \bar{v} \rangle^x + \langle v \rangle^x(z) + v'(x, z).$$

[Bryden and Imawaki (2001) refer to the first component as “barotropic,” but there is no connection with the normal implications of that term.] In sections with net mass transports (e.g., spanning the Circumpolar Current), the mass transports in the second and third terms on the right of (1) average to zero over the section area, so that they can be interpreted as heat transports, while the first term can only be interpreted as a temperature transport and so is arbitrary up to the choice of temperature zero.

Figure 7 shows such a decomposition of Eq. (1), when  $z$  is chosen as a neutral density coordinate. Heat is primarily transported by the overturning between shallow and deep density layers, except in regions of strong net

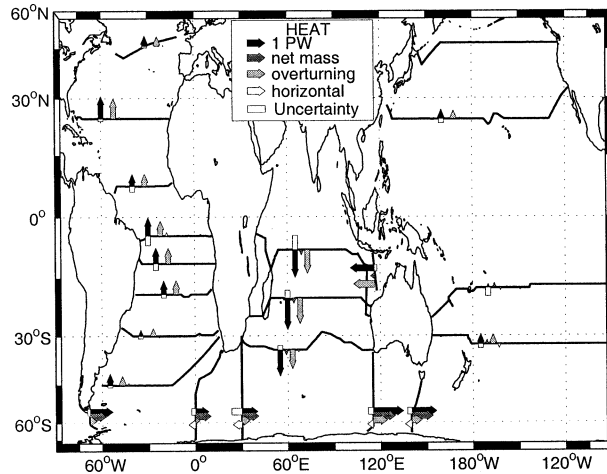


FIG. 7. Decomposition of heat transport in neutral density coordinates. The black arrow corresponds to the total transport, with contributions from the net mass transport across the section, from the overturning and from the horizontal correlations between temperature and velocities shown as the gray arrows.

mass transport such as the Southern Ocean. Note that the ITF appears to be dominated by the overturning in this diagnostic, because the section used is much deeper than the depth of the passage, showing that the decomposition is not very enlightening across that 117°E section. Figure 7 suggests that outside the Southern Ocean, a two-dimensional model in density coordinates is appropriate to represent heat transports, unlike the results for other property transports (see Ganachaud and Wunsch 2002).

Any decomposition is arbitrary and difficult to relate to physically meaningful processes. There have been for instance, debates about the distinction between the wind-driven circulation and the supposed “thermohaline” component (Wunsch 2002, manuscript submitted to *Paleoceanography*). As Bryden and Imawaki (2001) pointed out, in a decomposition in density coordinates, a strong, wind-driven boundary current such as the Gulf Stream carries large amounts of heat to the north, where it is cooled and it therefore returns to the south in layers of higher density. Although such a transport is wind driven, it corresponds to an overturning circulation. Quantitatively, with a reference temperature of 0°C, the energy transport of the Florida Current is of  $2.4 \pm 0.9$  PW to the north; the interior and Ekman flow at 24°N carry 1.1 PW to the south, for a total heat (mass conserving) transport of  $1.3 \pm 0.15$  PW. The partitioning of this circulation between elements that are wind driven and buoyancy driven is unknown, and as the dynamics are nonlinear, it is probably not possible to determine this, even in principle, from the fluxes themselves. Decompositions like these are useful kinematic/descriptive tools, but not easily related to driving forces.

Figure 8 gives a similar decomposition, but in depth coordinates. While the overturning component also dominates in the North Atlantic, the horizontal contri-

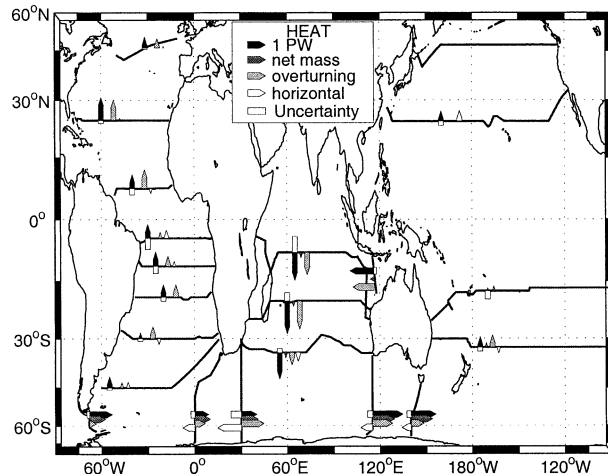


FIG. 8. Same as Fig. 7 but with a decomposition in pressure coordinates.

bution becomes increasingly important in the South Atlantic and south Indian Oceans and dominates the total transport in the North Pacific at 24°N, as noted by Bryden et al. (1991). In contrast, the salinity anomaly transports (Fig. 9), which are proportional to freshwater transports (see figure caption), are primarily horizontal, even in isopycnal coordinates. Horizontal transports most often dominate the total, while the overturning component can either exceed, or be in the opposite direction to the total. In pressure coordinates (not shown), the result is qualitatively similar except in the North Pacific at 24°N where both horizontal and overturning components are large and opposing, nearly canceling.

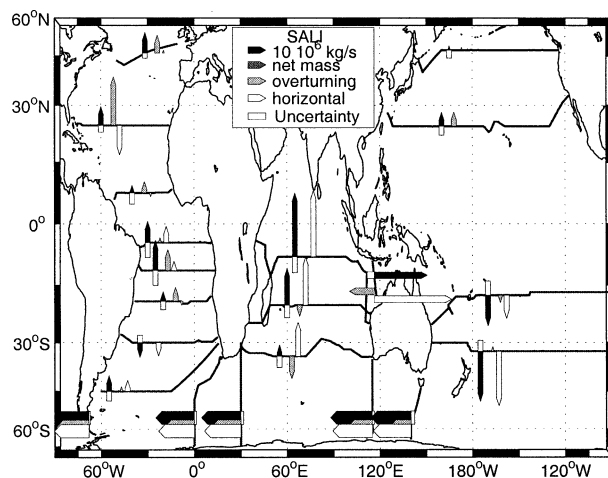


FIG. 9. Same as Fig. 7, but for transports of salinity anomaly with respect to the average salinity across the whole section. Transports of salinity anomalies are approximately equal to  $-35$  times the freshwater transports; a convergence of salinity anomaly being a net freshwater input to the ocean. The scale for thick arrows in the Southern Ocean is 10 times the scale for thin arrows. In regions of strong net mean flow such as the Southern Ocean, the transport of salinity anomaly is against the net salt transport. The effect of net mass transports is removed through the anomaly formulation (no arrow).



In conclusion, transports of heat and salt are made up of contributions from both horizontal (gyre) and meridional overturning circulations. Simplifications, such as omitting the zonal component as is done in two-dimensional ocean models will necessarily produce a transport that is wrong, almost everywhere, for freshwater and will also distort the heat transport in many locations.

## 6. Conclusions and outlook

Large-scale ocean–atmosphere exchanges of heat and freshwater from an inverse box model based on the WOCE hydrographic data are presented here and compared with independent flux products. Estimates are obtained for time-average transoceanic transports with realistic uncertainties. Consequently, the results are useful for the testing of bulk formula, atmospheric residual, and oceanic general circulation models. Heat transports are consistent within error bars with previous results from hydrographic data inversions—showing that we are finally obtaining convergence of the estimates. Formal comparison with flux products from residuals from meteorological reanalyses is difficult, as none of the published meteorological estimates is provided with a true error estimate. However, using our uncertainties as references, reasonable agreement is found with the adjusted NCEP-derived heat fluxes from TC except in the important high-latitude Northern Hemisphere. The ECMWF-derived products are generally less consistent, with an alarming difference between the lower boundary condition of ECMWF fields (Garnier et al. 2000) and the residuals estimated by TC. Freshwater transports from the inverse model are uncertain relative to heat transports, but still provide the only basin-scale reference values that include uncertainty estimates. Our comparison suggests that freshwater flux estimates from satellite radiometric data are too high in the Tropics—possibly due to the lack of adequate calibration. Residuals derived from NCEP and in situ observations are relatively consistent with ours everywhere—within the large uncertainties.

A decomposition of the transports in density and geopotential coordinates shows that heat and freshwater transports follow complex three-dimensional paths through the ocean—rendering difficult any simple generalization about dominant mechanisms. In particular, no two-dimensional model, whether in the depth–latitude or latitude–longitude planes, is likely to adequately represent the actual situation.

The remaining uncertainties in hydrographic estimates suggest several directions for future work. If the results are intended as estimates of the time average circulation, then the uncertainties are dominated by the temporal variability present in one-time hydrographic measurements. Repeat measurements are necessary to improve time averages, in particular in regions such as the Agulhas retroflexion where heat is transported by

transient processes. Also, full data-assimilating general circulation models as in Stammer et al. (2002) will reduce uncertainties by combining synoptic sections with a time-varying circulation.

Apart from the temporal sampling problem, several other improvements can be made. Better knowledge of the magnitude of the noise in the anomaly equations—and thus in the derived uncertainties of freshwater fluxes—can probably best be gained from simulations with high-resolution numerical ocean models (GAN). Regional analyses of the WOCE data will also help: the use of meridional sections outside the Southern Ocean would improve the spatial resolution, and the wider use of other types of data such as neutrally buoyant floats and acoustic Doppler current profiles (e.g., Wijffels et al. 2001) will reduce uncertainties. If regional calculations employing much more data of all types are produced with complete uncertainty estimates, one envisions a new global synthesis made from the combined regional products. In principle, such a synthesis would bring to bear all detailed knowledge about all elements of the ocean circulation everywhere.

Future hydrographic observations could be oriented so as to better serve the purpose of accurate flux estimates. Historically, many of the sections have been zonal, but, for example, a section between Florida and England would maximize the air–sea heat flux signal in the North Atlantic. Ekman transports, another major source of errors in our results, need to be better quantified. Oceanic wind fields are improving substantially with the arrival of scatterometer data, but their quantitative use will require an accompanying error estimate.

*Acknowledgments.* This paper was initially presented at the World Climate Research Program Workshop held in Washington in May 2001. Part of this work was done at the Laboratoire de Physique des Océans (IFREMER, Brest, France). Comments by B. Sloyan and two anonymous reviewers substantially helped to improve the manuscript. Supported in part by the U. S. National Ocean Partnership Program, the National Science Foundation, and by the Centre National d'Etudes Spatiales (France). This is a contribution to the World Ocean Circulation Experiment.

## REFERENCES

- Adler, R., C. Kidd, G. Petty, M. Morissey, and M. Goodman, 2001: Intercomparison of global precipitation products: The third precipitation intercomparison project (PIP-3). *Bull. Amer. Meteor. Soc.*, **82**, 1377–1396.
- Bacon, S., 1997: Circulation and fluxes in the North Atlantic. *J. Phys. Oceanogr.*, **27**, 1420–1435.
- Baumgartner, A., and E. Reichel, 1975: *The World Water Balance*. Elsevier Science, 179 pp.
- Bryden, H., and S. Imawaki, 2001: Ocean heat transport. *Ocean Circulation and Climate*, G. Siedler, J. Church, and J. Gould, Eds., Academic Press, 455–474.
- , D. H. Roemmich, and J. A. Church, 1991: Ocean heat transport across 24°N in the Pacific. *Deep-Sea Res.*, **38**, 297–324.

- da Silva, A., C. Young, and S. Levitus, 1996: Revised surface marine fluxes over the global oceans: The UWM/COADS data set. *WCRP Workshop on Air–Sea Flux Fields*, DYNAMO 1997 Science Rep. N2, Kiel, Germany, Institut für Meereskunde, 13–18.
- Ganachaud, A., and C. Wunsch, 2000: The oceanic meridional overturning circulation, mixing, bottom water formation, and heat transport. *Nature*, **408**, 453–457.
- , and —, 2002: Oceanic nutrient and oxygen transports and bounds on export production during the World Ocean Circulation Experiment. *Global Biogeochem. Cycles*, **16**, 1057 doi:10.1029/2000GB001333.
- , —, J. Marotzke, and J. Toole, 2000: The meridional overturning and large-scale circulation of the Indian Ocean. *J. Geophys. Res.*, **105**, 26 117–26 134.
- Garnier, E., B. Barnier, L. Siefridt, and K. Béranger, 2000: Investigating the 15 year air–sea flux climatology from the ECMWF reanalysis project as a surface boundary condition for ocean models. *Int. J. Climatol.*, **20**, 1653–1673.
- Hall, M. M., and H. L. Bryden, 1982: Direct estimates and mechanisms of ocean heat transport. *Deep-Sea Res.*, **29**, 339–359.
- Holfort, J., and G. Siedler, 2001: The meridional oceanic transports of heat and nutrients in the South Atlantic. *J. Phys. Oceanogr.*, **31**, 5–29.
- Hsiung, J., 1985: Estimates of global oceanic meridional heat transport. *J. Phys. Oceanogr.*, **15**, 1405–1413.
- Jackett, D. R., and T. J. McDougall, 1997: A neutral density variable for the world's oceans. *J. Phys. Oceanogr.*, **27**, 237–263.
- Jayne, S. R., and J. Marotzke, 2001: The dynamics of ocean heat transport variability. *Rev. Geophys.*, **39**, 385–411.
- Josey, S. A., E. C. Kent, and P. K. Taylor, 1999: New insights into the ocean heat budget closure problem from analysis of the SOC air–sea flux climatology. *J. Climate*, **12**, 2856–2880.
- Jourdan, D., P. Peterson, and C. Gautier, 1997: Oceanic freshwater budget and transport as derived from satellite radiometric data. *J. Phys. Oceanogr.*, **27**, 457–467.
- Kalnay, E., and Coauthors, 1996: The NCEP/NCAR 40-Year Reanalysis Project. *Bull. Amer. Meteor. Soc.*, **77**, 437–471.
- Keith, D. W., 1995: Meridional energy transport: Uncertainty in zonal means. *Tellus*, **47A**, 30–44.
- Klein, B., R. Molinary, T. Muller, and G. Siedler, 1995: A transatlantic section at 14.5°N: Meridional volume and heat fluxes. *J. Mar. Res.*, **53**, 929–957.
- Koltermann, K. P., A. Sokov, V. Terechtencov, S. Dobroliubov, K. Lorbacher, and A. Sy, 1999: Decadal changes in the thermohaline circulation of the North Atlantic. *Deep-Sea Res. II*, **46**, 109–138.
- Lavin, A., H. Bryden, and G. Parilla, 1998: Meridional transport and heat flux variations in the subtropical North Atlantic. *Global Atmos.–Ocean Syst.*, **6**, 269–293.
- Lux, M., and H. Mercier, 2001: Interhemispheric exchanges of mass and heat in the Atlantic Ocean in January–March 1993. *Deep-Sea Res. I*, **48**, 605–638.
- Macdonald, A., 1998: The global ocean circulation: A hydrographic estimate and regional analysis. *Progress in Oceanography*, Vol. 41, Pergamon, 281–382.
- , and C. Wunsch, 1996: An estimate of global ocean circulation and heat fluxes. *Nature*, **382**, 436–439.
- McDougall, T. J., 1991: Dianeutral advection. *Proc. Parameterization of Small-Scale Processes, Hawaiian Winter Workshop*, Honolulu, Hawaii, University of Hawaii at Manoa, 289–315.
- Rintoul, S. R., and C. Wunsch, 1991: Mass, heat, oxygen and nutrient fluxes and budget in the North Atlantic Ocean. *Deep-Sea Res.*, **38** (Suppl.), 355–377.
- Roemmich, D., J. Gilson, B. Cornuelle, and R. Weller, 2001: The mean and time-varying meridional transport of heat at the tropical/subtropical boundary of the North Pacific Ocean. *J. Geophys. Res.*, **106**, 8957–8970.
- Sato, O., and T. Rossby, 2000: Seasonal and low-frequency variability of the meridional heat flux at 36°N in the North Atlantic. *J. Phys. Oceanogr.*, **30**, 606–621.
- Saunders, P. M., and B. B. King, 1995: Oceanic fluxes on the WOCE A11 Section. *J. Phys. Oceanogr.*, **25**, 1942–1958.
- Sloyan, B. M., and S. R. Rintoul, 2000: Estimates of area-averaged diapycnal fluxes from basin-scale budgets. *J. Phys. Oceanogr.*, **30**, 2320–2341.
- , and —, 2001: The Southern Ocean limb of the global deep overturning circulation. *J. Phys. Oceanogr.*, **31**, 143–173.
- Speer, K. G., J. Holfort, T. Reynaud, and G. Siedler, 1996: South Atlantic heat transport at 11°S. *The South Atlantic: Past and Present Circulation*, G. Wefer et al., Eds., Springer-Verlag, 105–120.
- Stammer, D., and Coauthors, 2002: Global ocean circulation during 1992–1997, estimated from ocean observations and a general circulation model. *J. Geophys. Res.*, **107**, (C9), 3118, doi:10.1029/2001JC000888.
- Stommel, H., E. D. Stroup, and B. Warren, 1973: Trans-Pacific hydrographic sections at lats. 43°S and 28°S: The *Scorpio* expedition—I. Preface. *Deep-Sea Res.*, **20**, 1–7.
- Talley, L. D., 1984: Meridional heat transport in the Pacific Ocean. *J. Phys. Oceanogr.*, **14**, 231–241.
- Taylor, P., Ed., 2000: Intercomparison and validation of ocean–atmosphere energy flux fields. Final Report of the Joint WCRP/SCOR Working Group on Air–Sea Fluxes (SCOR Working Group 110), Tech. Rep. WCRP-112, WMO/TD-136, WMO, Switzerland, Geneva, 303 pp.
- Trenberth, K. E., and C. J. Guillemot, 1998: Evaluation of the atmospheric moisture and hydrological cycle in the NCEP/NCAR reanalyses. *Climate Dyn.*, **14**, 213–231.
- , and J. M. Caron, 2001: Estimates of meridional atmosphere and ocean heat transports. *J. Climate*, **14**, 3433–3443.
- , —, and D. Stepaniak, 2001: The atmospheric energy budget and implications for surface fluxes and ocean heat transports. *Climate Dyn.*, **17**, 259–276.
- Warren, B. A., 1999: Approximating the energy transport across oceanic sections. *J. Geophys. Res.*, **104**, 7915–7919.
- Wijffels, S., 2001: Ocean transport of fresh water, *Ocean Circulation and Climate*, G. Siedler, J. Church, and J. Gould, Eds., Academic Press, 475–488.
- , J. M. Toole, and R. Davis, 2001: Revisiting the South Pacific subtropical circulation: A synthesis of WOCE observations along 32°S. *J. Geophys. Res.*, **106**, (C9), 19 481–19 513.
- Worthington, L. V., and W. R. Wright, 1970: Potential temperature and salinity in the deep water including temperature, salinity and oxygen profiles from the Erika Dan cruise of 1962. *North Atlantic Ocean Atlas*, Woods Hole Oceanographic Institution, 6 pp., 58 plates, and data tabulation.
- Wunsch, C., 1996: *The Ocean Circulation Inverse Problem*. Cambridge University Press, 437 pp.